A new analytical formulation for the stiffness and resistance of the additional plate in bending in beam-to-beam steel joints.

Manuel Lopez[1], Alfonso Loureiro[1], Ruth Gutierrez[1], Jose M Reinosa[1]

[1]University of A Coruña

Laboratory of Structural Analysis. EPS Ferrol

Mendizabal s/n Campus de Esteiro 15403 Ferrol, Spain

Corresponding author: Manuel Lopez

E-mail address: manuel.lopez.lopez@udc.es

Tel.: +34 981337400; Fax: +34 981337410.

This is a post-peer-review, pre-copyedit version of an article published in Engineering Structures. The final authenticated version is available online at: https://doi.org/10.1016/j.engstruct.2020.111476 This document is licensed under a CC-BY-NC-ND license https://creativecommons.org/licenses/by-nc-nd/4.0/.

Abstract

This paper focuses on the stiffness and resistance of the additional plate in bending. This is a component which appears in beam-to-beam bolted steel joints, when a secondary beam with a flush end plate is attached orthogonally to the primary beam by an additional plate welded between its flanges. In this work, six experimental tests have been carried out to calibrate a finite element model which has been used to develop a wide parametric study. Thus, a new formulation for stiffness and resistance based on an equivalent frame is proposed.

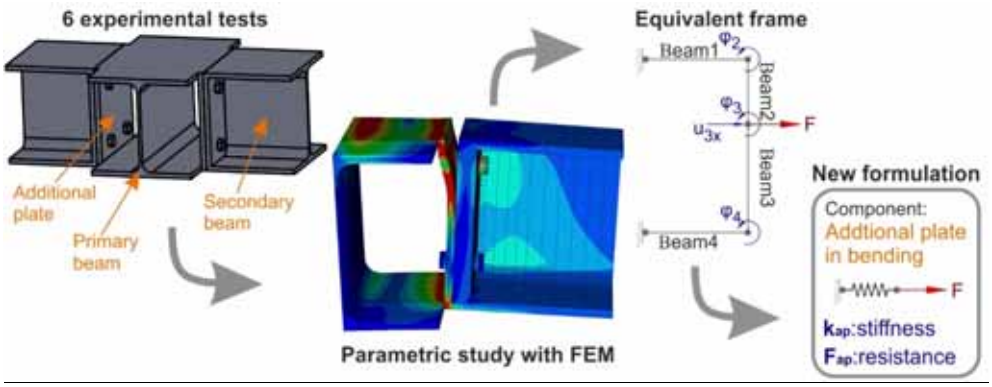

1. Introduction

Traditionally, steel joints have been considered pinned or rigid, although it is well known that semi-rigid behavior leads to more optimal structures. Different models – experimental, empirical, numerical, mechanical, analytical and informational [1] – could predict this behavior. One of the most popular mechanical models is the component method, which implies the assembling of the response of various basic individual springs called components which idealize each part of the joint. These components are modelled by means of stiffness and resistance. Many authors have carried out studies in this field to identify and characterize different components involved in most popular joints [2-9]. Much of this knowledge has been compiled in modern design codes like Eurocode 3 [10].

Extensive work has been made in beam-to-column joints subject to load in the major axis of the beam and in the minor axis [11-14]. Nevertheless, studies about beam-to-beam joints are less numerous, despite the fact that their influence is also relevant in many structure configurations [7, 15-17].

Urbonas and Daniūnas [7] have analyzed semi-rigid beam-to-beam end plate bolted joints subjected to bending and tension or compression axial force. They have suggested an extension of the component method to semi-rigid beam-to-beam end plate bolted joints under bending and axial force, which allows to obtain more accurate characteristics of the joints. The authors have also proposed an application to the analysis of framework structures with a simple iterative procedure [15].

Hawxwell and Tsvdaridisk [17] have also analyzed orthogonal beam-to-beam connections by an experimental campaign of three types of eccentric connections, the result of which shows that the eccentric end plate typology should be considered as semi-rigid. The other two typologies, the fin plate and partial-depth end plate, can be considered as nominally-pinned connections.

There are different ways to solve the orthogonal beam-to-beam connection. Traditionally, the web of the secondary beam can be welded directly to the web of the primary beam resulting in a pinned connection. In bolted connections, a flush end plate of secondary beam can be attached to a T shape stub welded to the flanges and web of the primary beam, resulting in a more stiff connection. However, the flush end plate of the secondary beam could be attached to the primary beam by an additional plate welded between the flanges of the primary beam (see Fig. 1). In this case, the connection could be pinned or semi-rigid depending on the dimensions of the joint parts.

Applying semi-rigid behavior in beam-to-beam joints leads us to safer structures because the torsion in the primary beam is taken into account. Furthermore, lighter structures could be reached using the semi-rigid joint response. This paper analyzes a beam-to-beam connection performed with an additional plate in the main beam and end plate in the secondary one attached by four bolts. Moreover, this type of connections is useful when the profile of the primary and secondary beam have the same height. If the secondary beam were smaller, the joint would be quite more flexible and could be considered pinned in most of the cases.

Eurocode 3 [10] compiles the most common components involved in the response of the joints. However, in this beam-to-beam typology, a new component appears that is the additional plate in bending, which represents the behavior of the additional plate welded between the flanges of the primary beam. Therefore, in order to use this new component in the component method, it is necessary to define its stiffness and resistance.

The aim of this article is to define an analytical formulation for stiffness and resistance of the component additional plate in bending that appears in this typology of beam-to-beam steel joints. This has been achieved in four steps: an experimental campaign of six tests, the development and calibration of a finite element model, a wide parametric study with the finite elements, and, in the last place, the development of a formulation for stiffness and resistance, from a matrix analysis of an equivalent frame.

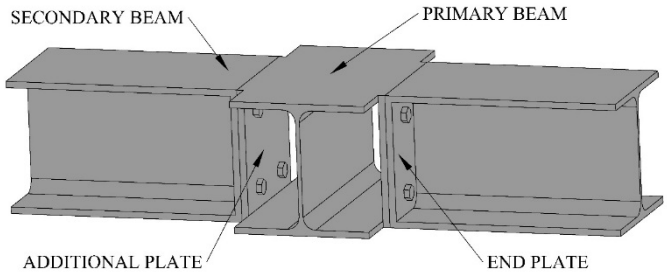

Fig. 1. Joint configuration.

2. Experimental program

The experimental work was designed in order to learn the influence of the additional plate in rotational behavior of the joint. Because of this, it is composed by 6 tests with different configurations as Table 1 shows. The primary and the secondary beam were equals and the profiles were type HEA but with different sizes. The nominal thickness of additional plates (t_{ap}) were 10, 15 and 20 mm; it should be observed that the real thickness of the third plate was 19.4 mm. The values *w* and *p* were the horizontal and vertical distance between bolts respectively.

The bolt distances were the same for each profile type with typical values for these profile sizes. Bolts were TR20 with quality 10.9 and HV system. They were chosen so as to avoid being the weak part of the joint. The same idea was adopted with the end plate of the secondary beams, which had a thickness of 30 mm in all cases. In the assembly of the joints, the bolts were hand-tightened up to ensure the snug-tight condition.

Test	Profile	t_{ap} (mm)	w (mm)	p (mm)	Bolts
B01	HEA 280	10	140	150	10.9 TR20
B02	HEA 280	15	140	150	10.9 TR20
B03	HEA 280	19.4	140	150	10.9 TR20
B04	HEA 200	10	100	90	10.9 TR20
B05	HEA 200	15	100	90	10.9 TR20
B06	HEA 200	19.4	100	90	10.9 TR20

Table 1. Experimental configurations.

Profile	t_{fb} (mm)	t_{wb} (mm)	h_b (mm)	b_b (mm)
HEA 280	11.5	8.85	271	277
HEA 200	8.8	7.0	193.5	204

Table 2. Real profiles dimensions.

Table 2 shows the real dimensions of the profiles obtained by the arithmetic mean of measurements in several points of the specimens. The parameter t_{fb} is the thickness of the column flange measured in the border, t_{wb} is the thickness of the web, h_b an b_b are the height and the width of the profiles respectively (see Fig. 2). The width of the additional plate was called b_{ap} and had the same value of the b_b of profile. Each profile type of the primary and secondary beam has been built from the same profile bar, which explains why they almost had the same dimensions. The length of the primary beam (l_{1b}) was 500 mm in all the tests, sufficiently long not to influence the joint behavior. The length of the secondary beam (l_{2b}) was 1000 mm in all cases.

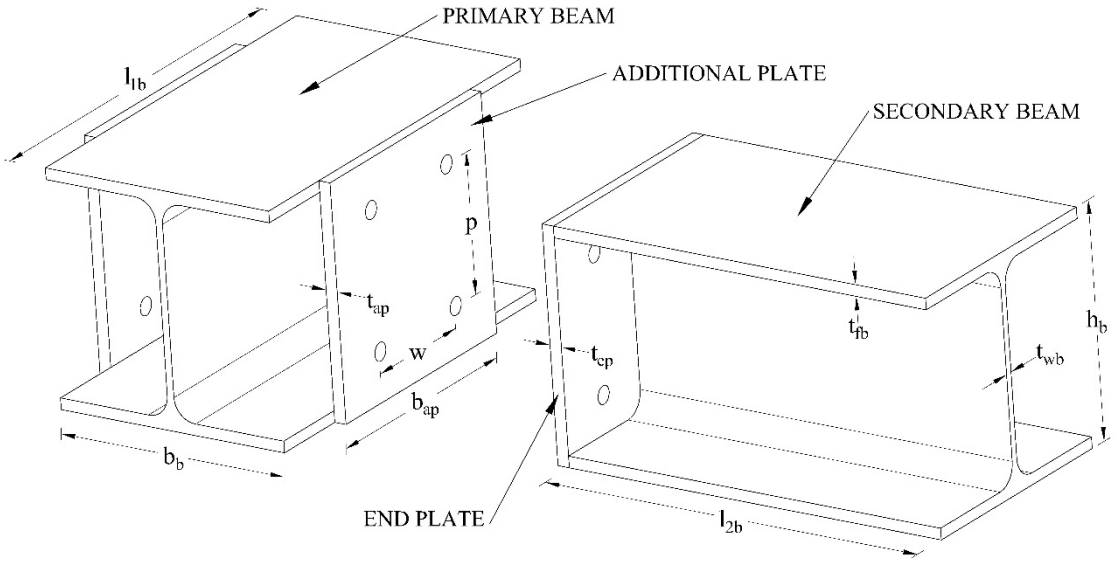

Fig. 2. Drawing of the primary and secondary beam.

The material of all parts of the specimens was S275 steel and coupons were extracted from the additional plates and the flange of the profiles to obtain true mechanical properties of the material. Table 3 shows those properties that will be used later in the finite element models for the calibration process.

Material	Yield stress (MPa)	Young's Module (MPa)
HEA 280	309	208647
HEA 200	321	211054
Plate 10 mm	307	210425
Plate 15 mm	295	208325
Plate 20 mm	297	207458

Table 3. Material properties.

2.1. Equipment and instrumentation

The main objective of the instrumentation is to obtain the moment-rotation curve. So, the tests were instrumented with a load cell and two inclinometers to measure the applied force and the rotation of the secondary beams. Moreover, strain gauges were placed in one of the additional plates as shown in Fig 3. A displacement sensor has been placed in the assembly with the aim of monitoring the evolution of the test and corroborate the inclinometer measurements. In all cases, a preloading step in the elastic range has been applied, and then, the specimens were loaded until the plastic behavior of the joint was reached.

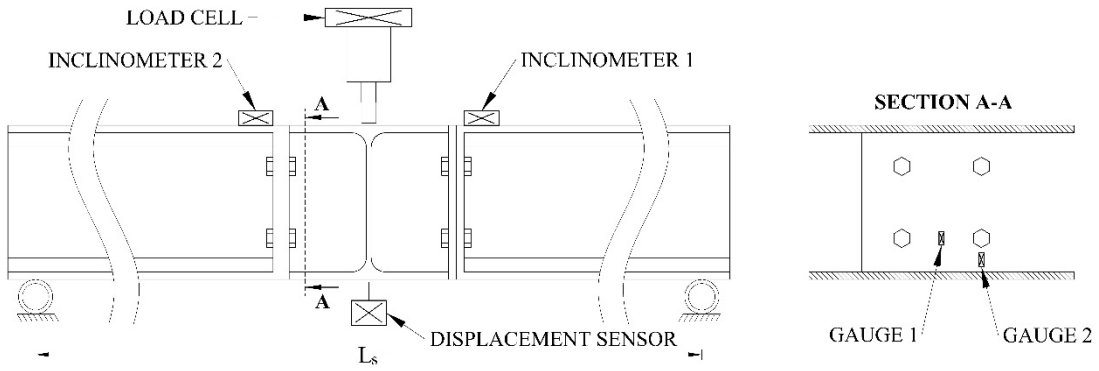

Fig. 3. Instrumentation. Section A-A shows the position of strain gauges.

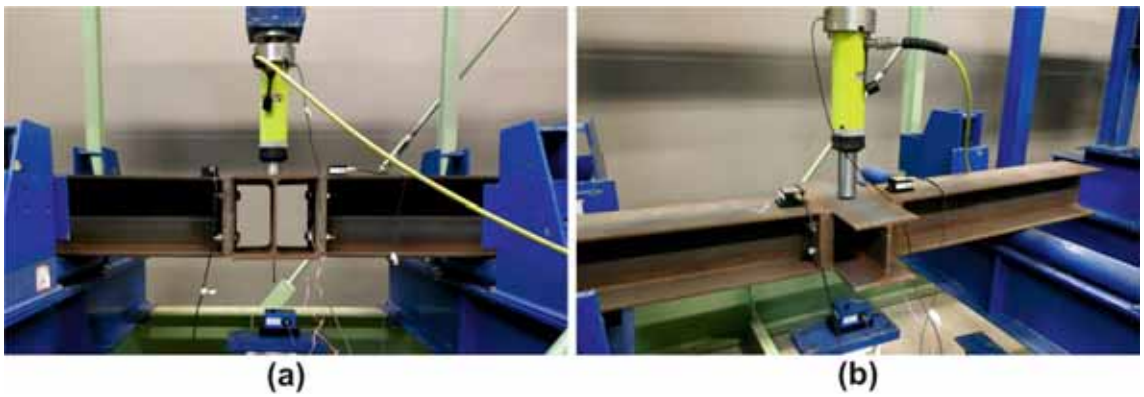

Fig. 4. (a) Frontal view of the Test B01 and (b) top view of the Test B05.

Each specimen represents two connections attached by the web of the primary beam, and because of this, the moment is half of the measured value of the load cell multiplied by the distance between the support and the additional plate. The rotation is the arithmetic mean of the measurements of the inclinometers 1 and 2. This average rotation helps to avoid imperfections in the tests, although both the rotation of inclinometer 1 and inclinometer 2 have had similar values in all of the tests. The distance between supports, called L_s in Fig. 3, was 1510 mm in all tests.

The measurements of the strain gauges were used to verify the yielding sequence of the additional plates. Due to deformation shape of the additional plates during the tests, in all cases gauge 1 was in compression and gauge 2 in tension. It should be noted that gauge 2 could not be placed in the tests B04, B05 and B06, because there was not enough space due to the size of the profile HEA200 and the vertical distance between bolts.

Fig. 4a and Fig. 4b show photographs of tests B01 and B05 respectively, where all the instrumentation can be seen. The load cell was placed between the hydraulic jack and the supporting structure (see Fig 4a) and the inclinometers were placed on the top of the

secondary beams (see Fig 4b). Fig 5 shows the deformation of the tests B02, B03, B04 and B06. The influence of the thickness of the additional plate in the connection can be seen comparing the deformation measurements of the tests B02 and B03 (Fig. 5a and 5b) and between B04 and B06 (Fig. 5c and 5d).

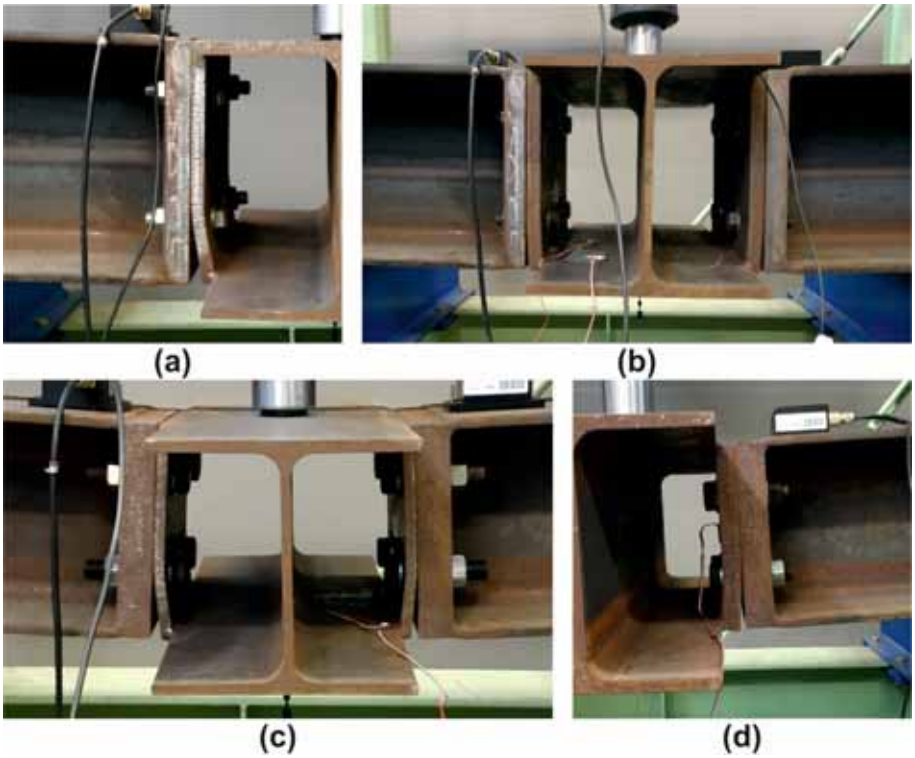

Fig. 5. Deformation of the additional plate in tests: (a) B02, (b) B03, (c) B04 and (d) B06.

3. Finite element models

3.1. Geometry, elements and boundary conditions

The finite element models were performed using Abaqus® Standard. The type of element adopted was C3D8R, which is a solid element with 8 nodes, reduced integration and hourglass control. Fig. 6 shows the typical numerical model in which the different parts are represented by different colors. This model takes the advantage of the symmetry and only a quarter of the connection was modeled. The real mechanical properties of the material showed in Table 3 were introduced in the finite element model. In the case of bolts, nominal values of TR10.9 were used. The inelastic behavior of the material was considered by Von Misses yield criterion associated with a three linear stress-strain relationship to incorporate strain hardening. The static analysis was performed by displacement control applied to the primary beam; moreover, nonlinearities of material and geometry were taken into account.

The assembly of the model has five different parts: primary beam with the additional plate, secondary beam, end plate, bolts and washers. Contacts have been modeled between the

following pairs: end plate-additional plate, washers-end plate, washers-additional plate, bolt shank-additional plate, bolt shank-end plate, bolt shank-washers, washer-bolt head and washer-nut. The normal behavior was modeled as hard contact and the tangential behavior with a friction coefficient of 0.25. These surfaces were allowed to be separated after contact. The end plate and secondary beam were joined by a tie constraint.

3.2. Mesh

All models have a quite refined mesh obtained after a convergence study (see Fig. 6), based on previous works [14, 18-20] and comparative models. These models have been done with different mesh sizes, which became decisive in matching the experimental results. The element size is different depending on whether the part is a main source of deformation or not, and on the involved contacts. The additional plate and the flange of primary beam close to it have elements with an approximated size of 3.5 mm. However, in the case of the secondary beam and the parts of the primary beam far away from the additional plate, the element size is around 20 mm. The end plate was modeled with an element size of 5 mm to assure a good contact with the shank of the bolt. In the same way, the elements of the bolts and washers have an approximated size of 2 mm mainly to assure a correct contact in all of their surfaces.

In the FEM (Fig. 6), the bolt and the nut were modeled together in one part [20]; moreover, the bolt shank was modeled with the nominal section. This leads to a lesser computational effort and makes convergence easier. More precise and complex models could be adopted for bolts and nuts [21, 22], but the aim of this article is to obtain the bending behavior of the additional plate.

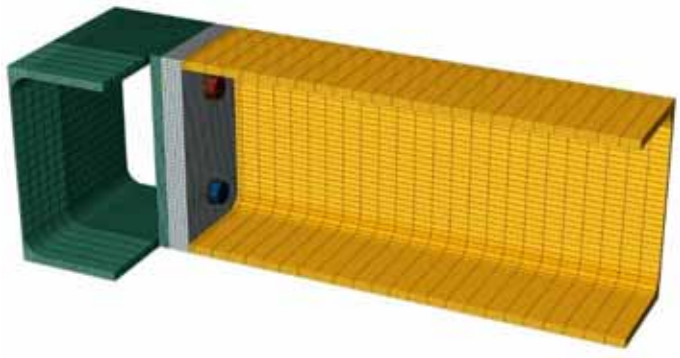

Fig. 6. Parts and mesh of the finite element model.

3.3. Calibration of the finite element models

The calibration of the finite element models is based on both the moment-rotation and moment-strain curves. The rotation in the finite element model was measured in the same

position where the inclinometers were placed on the secondary beam in the tests (see Fig. 3 and Fig. 4b). The strain in finite element models was measured in the same position where the strain gauges were placed on the additional plates of the tests (see Section A-A of Fig.3).

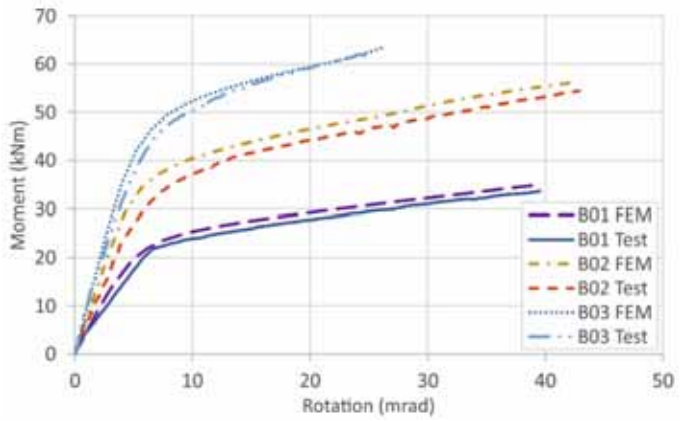

Fig. 7. Moment-rotation curves for B01, B02 and B03.

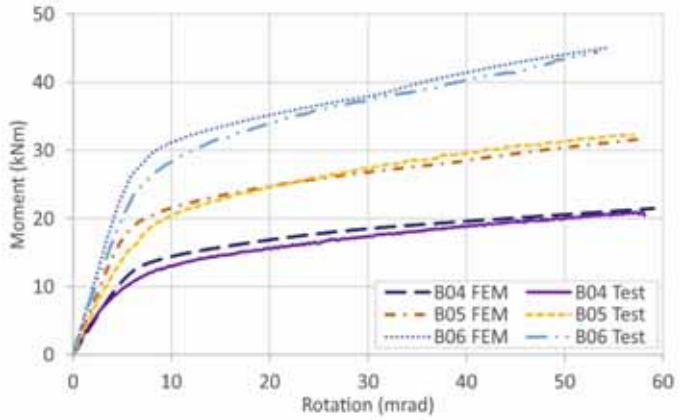

Fig. 8. Moment-rotation curves for B04, B05 and B06.

The moment rotation curves of the first three tests B01 to B03, corresponding with the beam profile HE280A, are depicted in Fig. 7. The graph shows the influence of the additional plate thickness in the stiffness and resistance. Moreover, the finite element models are able to fit the behavior of the tests quite accurately, both in the elastic and plastic ranges. Fig. 8 shows the moment rotation curve of tests B04 to B06 compared with the corresponding finite element models. Like in first ones, the finite element models fit the experimental behavior with good accuracy.

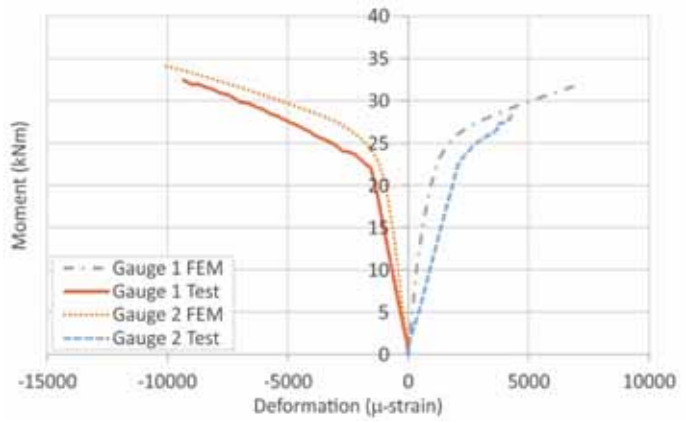

Fig. 9. Moment-strain curves of B01.

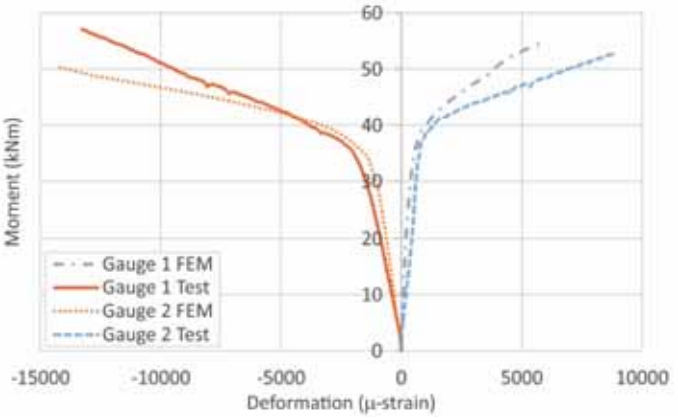

Fig. 10. Moment-strain curves of B02.

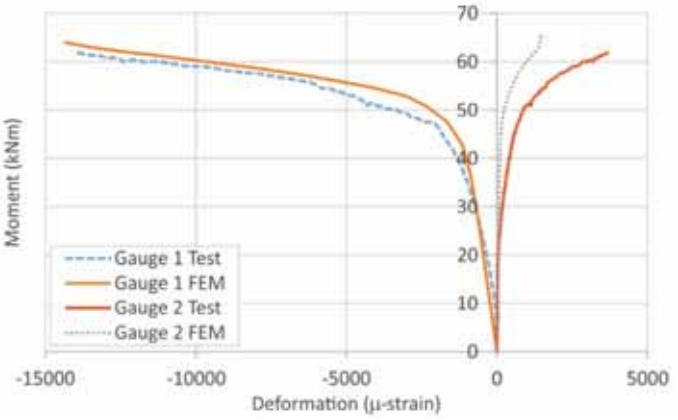

Fig. 11. Moment-strain curves of B03.

Figs. 9 to 11 show a comparison of the measurements of gauges 1 and 2 in tests B01, B02 and B03 and their respective strain measurements in the finite element models. The graphs show that the strain behavior of the models correspond with those of the tests both in the elastic and plastic ranges. Note that gauge 1 is in compression and gauge 2 is in tension in all of the tests due to the deformation mode of the additional plate. In test B01 gauge 2 failed before the end of the test.

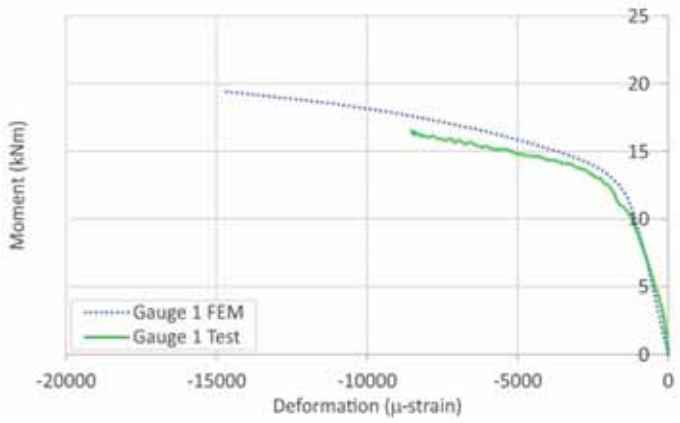

Fig. 12. Moment-strain curves of B04.

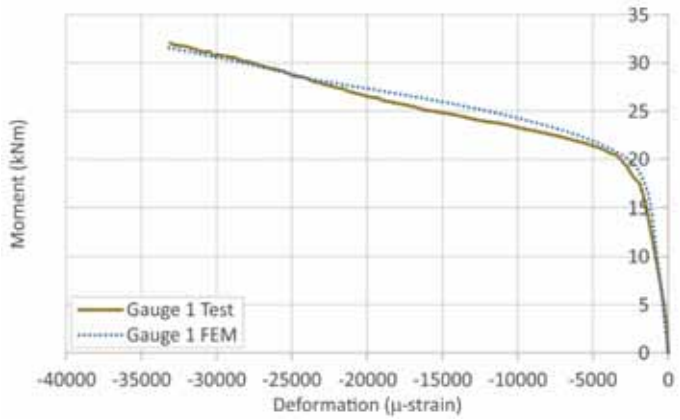

Fig. 13. Moment-strain curves of B05.

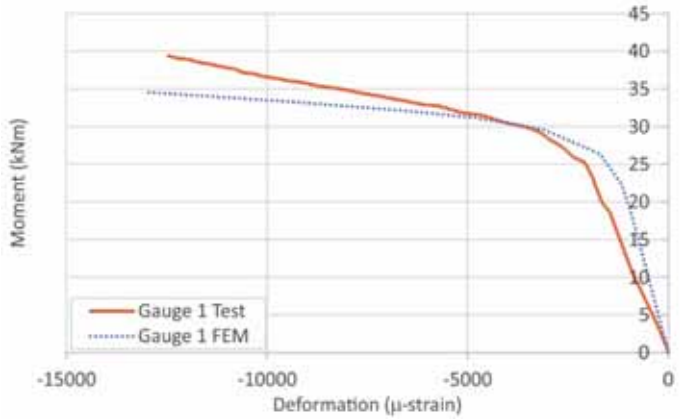

Fig. 14. Moment-strain curves of B06.

Fig. 12 to 14 show a comparison of gauge 1 in tests B04, B05 and B06 and the respective results of the finite element models. Like in the first three tests, the finite element models fit with good accuracy the strain behavior of the tests in the position of gauge 1. In B04 and B06 the gauges failed before the end of the test.

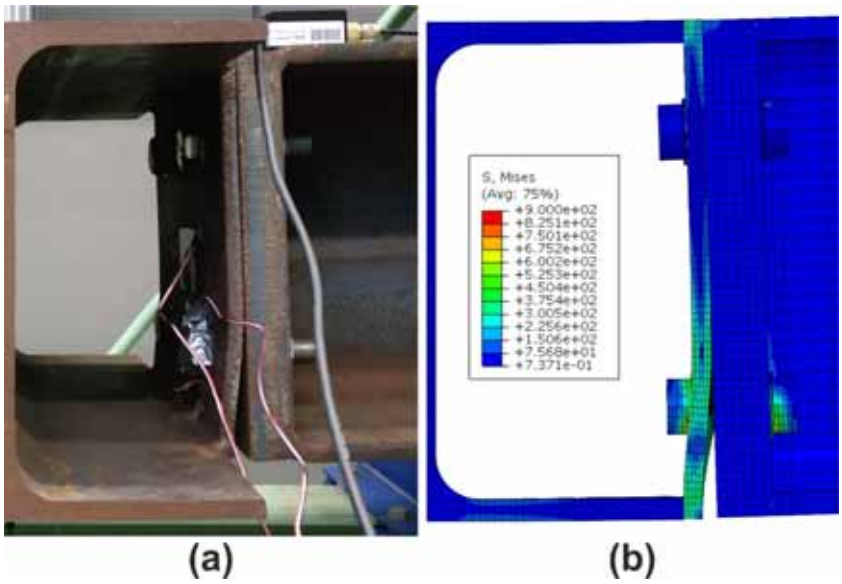

Fig. 15. Deformation comparative of B01. (a) Test and (b) finite element model.

Fig.15 shows a comparative image of the deformation for B01 test (Fig. 15a) and its respective finite element model (Fig. 15b). A good agreement between them can be observed in all of the parts involved in the joint. Therefore, the finite element model is able to reproduce the behavior of the joint with good accuracy.

4. Analytical characterization of the joint

From the experimental tests and finite element models, it can be observed that the major deformation and stress take place in the additional plate and specifically in its tensioned area. Fig. 16 shows the Von Misses stress of the primary beam and the additional plate of the finite element model of B01 with a deformation scale factor of 10. Similar results have been obtained in all models, showing that the additional plate is the main source of the deformation and therefore, the most influencing element in the evaluation of the stiffness and resistance of this type of joints.

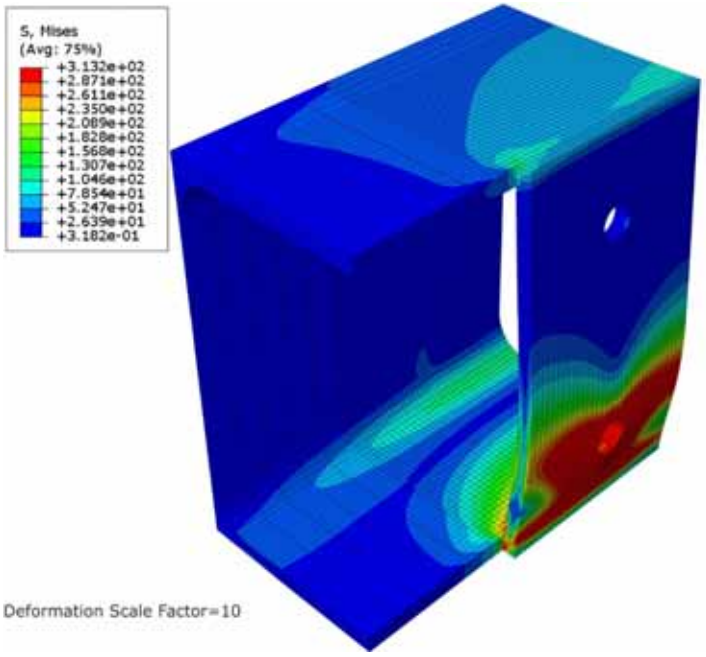

Fig. 16. Von Misses stress of B01 finite element model.

4.1. Parametric study

In order to study the behavior of the additional plate, a parametric study with finite element models has been carried out by means of the software Abaqus®. The parametric study consists of 288 models, as summarized in Table 4. In this study 12 different beam profiles (6 HEA and 6 IPE sections) called submodels ME01 to ME12 were studied. For each of these submodels there are 2 different values for horizontal distance between bolts (*w*), 2 vertical distances between bolts (*p*), 3 different values of thickness of the additional plate (t_{ap}) and 2 different types of bolts. These combinations led to 24 different cases in each subgroup of models. In all cases, the end plate has a thickness of 30 mm in order to minimize its influence in the joint behavior. Moreover, the additional plate and end plate have the height and width of the beam profiles.

Submodel	**Profile**	**w(mm)**		**p(mm)**		**t_{ap}(mm)**			**Bolt**	
		w1	**w2**	**p1**	**p2**	**t_{ap}1**	**t_{ap}2**	**t_{ap}3**	**Bolt1**	**Bolt2**
ME01	HE200A	50	100	130	100	8	10	12	10.9TR16	10.9TR20
ME02	HE240A	60	120	160	110	10	12	15	10.9TR16	10.9TR20
ME03	HE280A	70	140	200	150	10	12	15	10.9TR16	10.9TR20
ME04	HE300A	75	150	220	170	10	12	15	10.9TR16	10.9TR20

ME05	HE400A	70	200	300	250	15	18	20	10.9TR16	10.9TR20
ME06	HE450A	80	210	350	300	18	20	22	10.9TR16	10.9TR20
ME07	IPE180	50	60	120	100	8	10	12	10.9TR16	10.9TR20
ME08	IPE200	50	65	140	110	8	10	12	10.9TR16	10.9TR20
ME09	IPE240	55	70	175	150	8	10	12	10.9TR16	10.9TR20
ME10	IPE300	60	80	230	180	8	10	12	10.9TR16	10.9TR20
ME11	IPE400	60	100	320	270	10	12	15	10.9TR16	10.9TR20
ME12	IPE450	60	100	370	320	10	12	15	10.9TR16	10.9TR20

Table 4. Models of the parametric study.

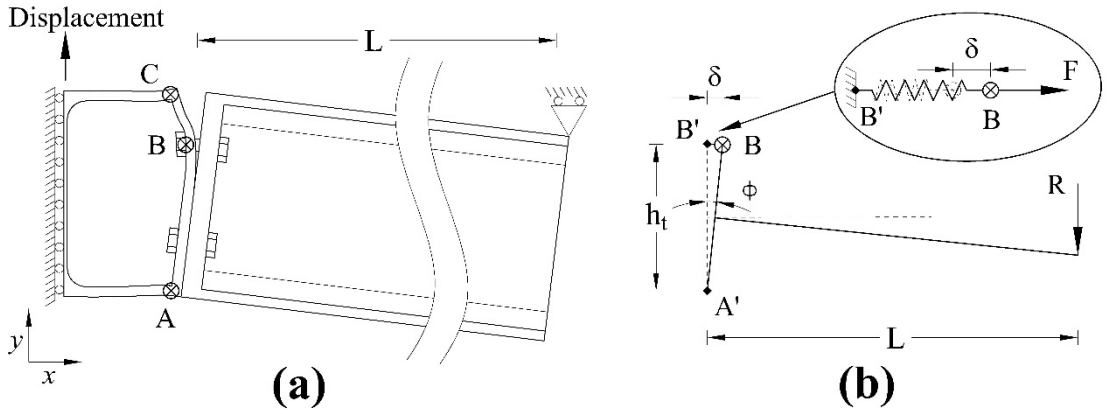

Fig. 17. Reference points in deformed model (a) model view and (b) schematic view.

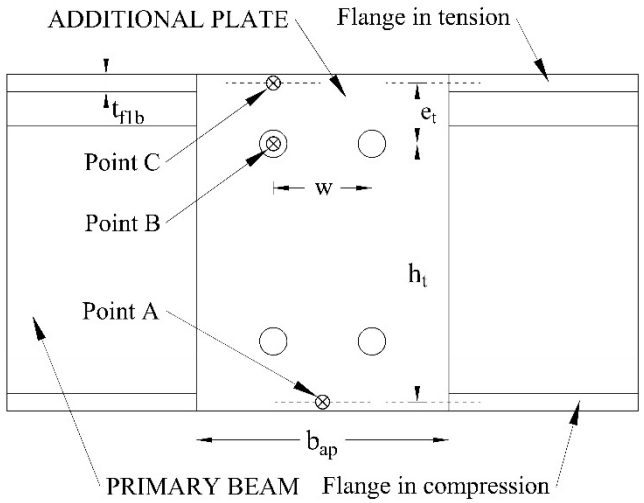

Fig. 18. Parameters and reference points in the primary beam and in the additional plate.

The data obtained from the parametric study was the horizontal displacement of the additional plate in the position of the more tensioned bolt line, which corresponds with point

B, as can be seen in Fig. 17a. Fig 17b shows a schematic view of the finite element model where R is the reaction force in the support and L is the length of the secondary beam plus the thickness of its end plate. To obtain the net displacement of point B, called δ in Fig. 17b, the displacement of the points A and C have to be taken into account as shown in Eq. 1.

$$\delta = u_{Bx} - \left(\frac{u_{Cx}-u_{Ax}}{h_t+e_t} h_t + u_{Ax}\right) \quad (1)$$

Where u_{Ax} is the horizontal displacement of the point A, located in the middle of the flange in compression and in the middle of the additional plate. u_{Bx} is the horizontal displacement of the bolt measured in a node in the center of the section between the head and the shank. u_{Cx} is the horizontal displacement of a point placed in the middle of the flange in tension just over the bolt. The parameter e_t is the distance between the bolt line with more tension and the center of the flange in tension and h_t is the distance between this bolt line to the center of the flange in compression (see Fig. 17 and Fig. 18). In the detail view of Fig.17b, the component additional plate in bending is represented as a spring. The bending moment applied to the joint leads to an equivalent force in the bolt, *F*, that produces the mentioned displacement of this spring, δ. The relationship between this force and the corresponding displacement, characterizes the stiffness and the resistance of the additional plate in bending.

The results obtained from the parametric study are shown in the table of the Appendix.

4.2. Characterization of the component additional plate in bending

In the component method the parameters that characterize each component are stiffness and resistance. In order to obtain these parameters for the additional plate in bending, an equivalent frame was adopted as the mechanical model to reproduce its behavior. Loureiro et al. have adopted similar idealization for the characterization of the E-stub in [18] and [19] with very good results. Fig. 19 shows the equivalent frame adopted in the present study, where 4 beams reproduce the behavior of the plate. Beam 2 and 3 represent the behavior of the additional plate; Beam 1 and 4 represent the influence of the flanges of the primary beam in the additional plate behavior. When a moment *M* is applied in the secondary beam, the equivalent frame is loaded by a force *F* in the point 3, transmitted by the most loaded bolts line. The influence of the other bolts line can be neglected as it can be seen in the stress distribution of the finite element models (see Fig 15 and 16), where the bolt and the area of the additional plate around the hole have little stress. Therefore, this bolts line does not have relevant influence in the bending behavior of the additional plate. The obtained results in the parametric study reinforce this assumption.

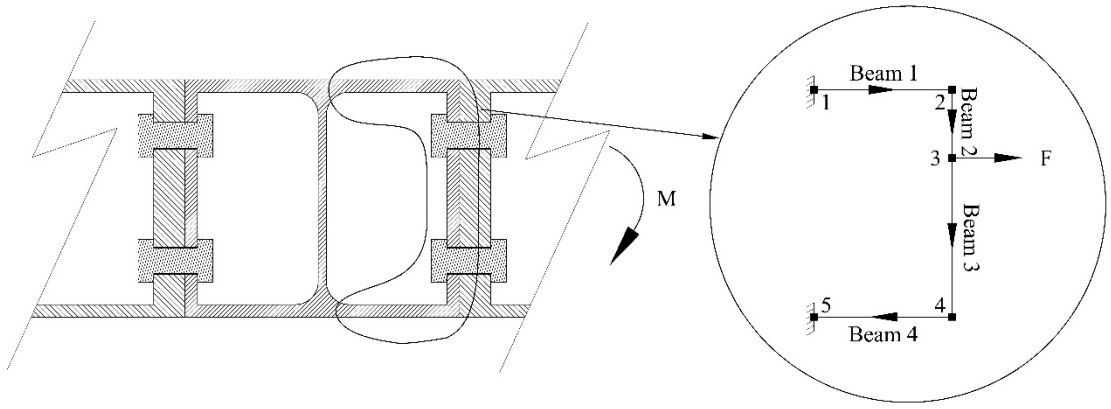

Fig. 19. Equivalent frame as mechanical model for additional plate in bending.

Fig. 20 shows the 4 degrees of freedom that have been taken into account in this equivalent frame. φ_2 corresponds to the rotation in point 2. φ_3 and u_{3x} are the rotation and horizontal displacement of point 3 respectively. φ_4 corresponds with the rotation in point 4. Other degrees of freedom are neglected because they are relatively small compared with the mentioned 4 degrees of freedom. The length of beams are *h* for Beam 1 and 4, while *m* and *n* are the lengths of Beams 2 and 3, respectively.

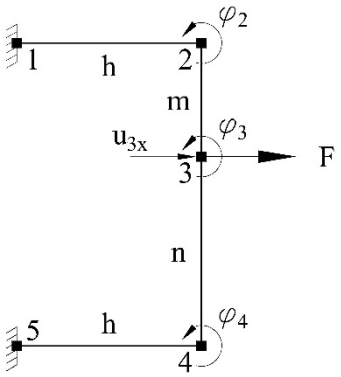

Fig. 20. Parameters and degrees of freedom of the equivalent frame.

To evaluate the stiffness of the equivalent frame, considering only the named 4 degrees of freedom, the individual stiffness matrices of the four beams should be assembled in the global stiffness matrix as shown in Eq. 2. Where in each member of the matrix, the subscript indicates the degree of freedom of the individual stiffness matrix and the superscript the reference number of the beam.

$$\underline{K} = \begin{bmatrix} K_{66}^{1} + K_{33}^{2} & K_{35}^{2} & K_{36}^{2} & 0 \\ K_{53}^{2} & K_{55}^{2} + K_{22}^{3} & K_{56}^{2} + K_{23}^{3} & K_{26}^{3} \\ K_{63}^{2} & K_{65}^{2} + K_{32}^{3} & K_{66}^{2} + K_{33}^{3} & K_{36}^{3} \\ 0 & K_{62}^{3} & K_{63}^{3} & K_{66}^{3} + K_{33}^{4} \end{bmatrix} \tag{2}$$

The vector of the applied forces contains only the force *F* applied at point 3 as shown in Eq. 3 and the vector of degrees of freedom can be seen in Eq. 4. Hence, Eq. 5 is the matrix equation of the equivalent frame.

$$\vec{F}^T = [0 \quad F \quad 0 \quad 0] \tag{3}$$

$$\vec{\delta}^T = [\varphi_2 \quad u_{3x} \quad \varphi_3 \quad \varphi_4] \tag{4}$$

$$\vec{F}^T = \underline{K}\vec{\delta}^T \tag{5}$$

Solving the Eq.5, the stiffness of the equivalent frame in point 3 can be obtained by dividing the force *F* by the displacement u_{3x}, leading to the expression of the stiffness of the additional plate in bending shown in Eq. 6.

$$k_{ap} = \frac{3EI_1l^2\left(3h^2I_1^2+8hI_2I_1l+4I_2^2l^2\right)}{n^2m^2\left(3h^2I_1^2l+4I_2^2nml+hI_2I_1(3n^2+8nm+3m^2)\right)} \tag{6}$$

Where, *E* is Young's module of the additional plate, I_1 is the inertial moment of Beam 2 and Beam 3 (see Eq. 7), I_2 is the moment of inertia of Beam 1 and Beam 4 (see Eq. 8) and *l* is the total length of Beam 2 plus Beam 3 (see Eq. 9).

$$I_1 = \frac{1}{12} b_{eff,k} t_{ap}^3 \tag{7}$$

$$I_2 = \frac{1}{12} b_{eff,f,k} t_{f1b}^3 \tag{8}$$

$$l = n + m \tag{9}$$

The parametric study leads to a length of Beam 2 indicated in Eq. 10. Where h_{1b} and t_{f1b} are the height and flange thickness of the primary beam, respectively and d_h is the diameter of the bolt head. Eq. 11 defines the height of Beam 3. The height of Beam 1 and Beam 4 is defined by Eq. 12. Where b_{1b}, t_{w1b} and r_{1b} are the width, web thickness and root radius of the primary beam, respectively.

$$m = \left(\frac{h_{1b}-t_{f1b}-p}{2}\right) + \frac{2}{\sqrt{3}}\left(t_{ap} - \frac{d_h}{4}\right) \tag{10}$$

$$n = \left(h_{1b} - t_{f1b}\right) - m \tag{11}$$

$$h = \frac{b_{1b}}{2} - \frac{t_{w1b}}{2} - 0.8r_{1b} + \frac{t_{ap}}{2} \tag{12}$$

Eq. 13 defines $b_{eff,k}$ that is the effective width of Beams 2 and 3 to evaluate the stiffness of the additional plate. It was obtained by means of a regression analysis from the models of the

parametric study. Eq. 14 defines the effective width of Beam 1 and 4, called $b_{eff,f,k}$, that is the effective width $b_{eff,k}$, plus a dispersion with an angle of 30 degrees along the length h.

$$b_{eff,k} = 0.63\left(\pi d_h + 2p + \frac{w}{2} + \min\left(m + d_h; \frac{b_{ap}}{2}\right)\right)\sqrt{\frac{b_{ap}}{h_{1b}}} \quad (13)$$

$$b_{eff,f,k} = b_{eff,k} + h\tan 30^{\circ} \quad (14)$$

To validate the formulation for stiffness formulation proposed in Eq. 6, the results of the stiffness of the parametric study obtained with the finite element models and those obtained by means of the proposed formulation are compared in Fig. 21. Where $k_{ap,FEM}$ is the stiffness of the finite element models and k_{ap} the stiffness of the equivalent frame defined by Eq. 6. Analyzing these results, the average of the factor $k_{ap,FEM}/k_{ap}$ is 1.003 and its standard deviation is 0.053. The maximum error in percentage is 17.0%. These results show the good accuracy of the proposed formulation for stiffness of the additional plate. The numerical results of all models of the parametric study can be seen in the Table of the Appendix.

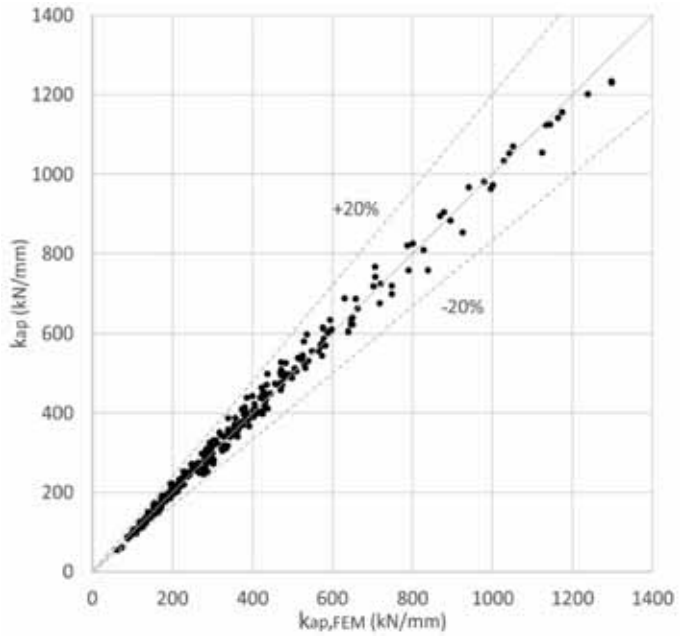

Fig. 21. Stiffness comparison between FEM and proposed formulation.

To evaluate the resistance of the additional plate in bending, it is considered that a plastic hinge is developed in Point 3 of the equivalent frame (see Fig. 22). This point corresponds with the node of application of the force transmitted by the bolts line with more tension. Looking at the stress distribution in the finite element models, it can be seen that there is a concentration of stresses in the area of the more tensioned bolts line (see Fig. 16). This area corresponds with point 3 of the equivalent frame.

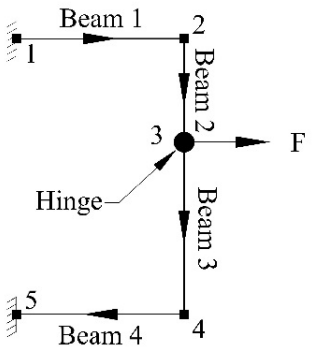

Fig. 22. Placement of the hinge in the equivalent frame.

The force *F* that develops a plastic hinge in Point 3 can be obtained by solving the matrix problem proposed in Eq. 5, and the global displacements of the equivalent frame can be defined as shown in Eq. 15.

$$\vec{\delta}^T = \underline{K}^{-1}\vec{F}^T \tag{15}$$

This global displacements vector can be transformed into the local displacements of Beam 2 as Eq. 16 shows.

$$\vec{\delta}_2^T = [0 \quad 0 \quad \varphi_2 \quad 0 \quad u_{3y} \quad \varphi_3] \tag{16}$$

Hence, if $\underline{K_2}$ is the stiffness matrix of Beam 2, the vector of nodal forces of Beam 2, $\vec{F}_2$, can be expressed as indicated in Eq. 17 and 18.

$$\vec{F}_2^T = \underline{K_2}\vec{\delta}_2^T \tag{17}$$

$$\vec{F}_2^T = [F_{1x} \quad F_{1y} \quad M_1 \quad F_{2x} \quad F_{2y} \quad M_2] \tag{18}$$

In the vector of forces defined in Eq. 18, when M_2 reaches the ultimate moment of the section of Beam 2, a plastic hinge is developed in Point 3. Therefore, the force *F* that produces the ultimate moment can be evaluated by Eq. 19. This force *F* is now called $F_{ap,Rd}$ that is resistance of the additional plate in bending.

$$F_{ap,Rd} = M_{pl,Rd}\frac{l^2(3h^2I_1^2+8h\mathrm{I}_1\mathrm{I}_2l+4I_2^2l^2)}{mn(3h^2{\mathrm{I}_1}^2l+8I_2^2mnl+4h\mathrm{I}_1\mathrm{I}_2(m^2+3mn+n^2))} \tag{19}$$

Where $M_{pl,Rd}$ is the ultimate moment defined in Eq.20 and $f_{y,ap}$ is the yield strength of additional plate.

$$M_{pl,Rd} = 0.25b_{eff,F}f_{y,ap}t_{ap}^3 \tag{20}$$

Eq. 21 defines the moment of inertia of Beam 2 and 3. For Beam 1 and 4, the moment of inertia is defined in Eq. 22.

$$I_1 = \frac{1}{12} b_{eff,F} t_{ap}^3 \tag{21}$$

$$I_2 = \frac{1}{12} b_{eff,f,F} t_{f1b}^3 \tag{22}$$

Where $b_{eff,F}$ is the effective width of the Beams 2 and 3. It has been obtained by regression analysis from the results of the finite elements models of the parametric study and is defined by Eq. 23. $b_{eff,f,F}$ is the effective width for Beams 1 and 4 and is defined by Eq. 24. This width is $b_{eff,F}$ plus a stress dispersion along the length h with an angle of 30 degrees. Note that these effective widths are different from the other ones used in the stiffness evaluation.

$$b_{eff,F} = 0.95 \left(\frac{\pi d_h}{2} - \frac{p}{6} + \frac{w}{2} + 3 \min \left(m + d_h; \frac{b_{ap}}{2} \right) \right) \sqrt{\frac{b_{ap}}{h}} \tag{23}$$

$$b_{eff,f,F} = b_{eff,F} + h \tan 30^{\circ} \tag{24}$$

In order to validate the formulation presented for the resistance in Eq. 19, the results of this expression are compared with the results extracted from the finite elements models of the parametric study (see Fig. 23). Where $F_{ap,Rd,FEM}$ is the resistance from the finite element models and $F_{ap,Rd}$ the resistance from the equivalent frame using Eq. 19. Analyzing these results the average of the factor $F_{ap,Rd,FEM}/F_{ap,Rd}$ is 1.011 and its standard deviation is 0.073. The maximum error in percentage is 21.1%. These statistical data indicate that the proposed formulation for the resistance of the additional plate in Eq. 19 is accurate enough. In this comparative, 28 models of the parametric study have not been taken into account because they do not develop completely the plastic behavior before the bolts yielding, which means that these models are not adequate for characterizing the strength of this component. These models can be identified in the table of the Appendix because they do not have values of resistance.

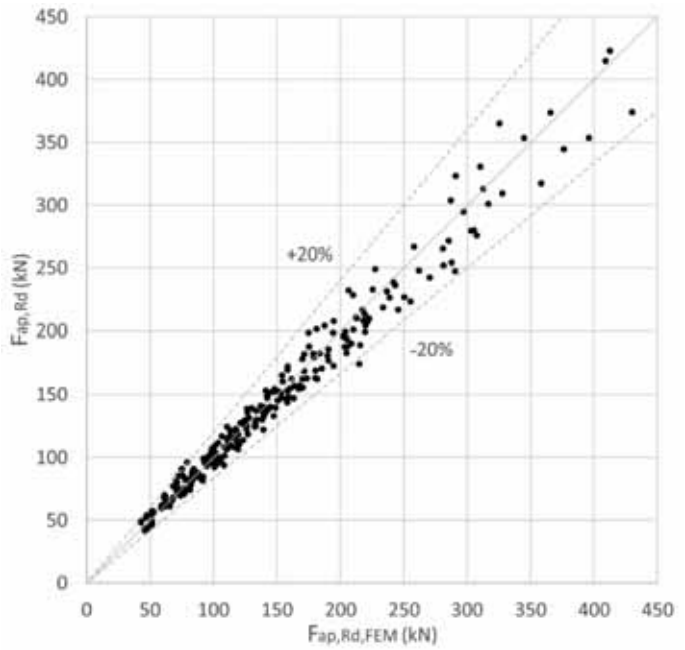

Fig. 23. Resistance comparison between FEM and proposed formulation.

5. Summary and conclusions

- Beam-to-beam orthogonal steel joints can be solved by attaching the end plate of the secondary beam to an additional plate welded between the flanges of the primary beam. In this case, a new component appears, which is not covered by the Eurocode 3. The component can be called additional plate in bending.
- In this work six experimental tests of beam-to-beam joints have been carried out and the moment-rotation curves of the secondary beam and the moment-deformation curves of the strain gauges have been obtained.
- Numerical finite element models have been developed. These numerical models have been calibrated with the experimental test. The validation of the models were carried out by the comparison of the moment-rotation curves of the joints and the moment-deformation curves of the strain gauges, showing that finite element models are able to reproduce the results of the test with great accuracy.
- The analytical characterization of the joints shows that the additional plate in bending is the most relevant component by its contribution to stiffness and resistance. This component is not covered by the Eurocodes.
- A wide parametric study of 288 geometries has been carried out by means of calibrated finite element models.
- A mechanical model based in an equivalent frame of the additional plate in bending was developed to predict the stiffness and resistance of this component. An analytical formulation for the stiffness and resistance, based in structural matrix analysis was

proposed. This formulation was compared with the results of the parametric study showing that the equivalent frame is able to predict the stiffness and resistance with enough accuracy.

- With the proposed formulation for stiffness and resistance, this new component, called additional plate in bending, is completely defined and could be used along with the traditional component method.

Acknowledgments

The financial support provided by the Spanish Ministerio de Economía y Competitividad and Fondo Europeo de Desarrollo Regional under contract BIA2016-80358-C2-2-P MINECO/FEDER UE is gratefully acknowledged.

References

[1] Díaz C, Martí P, Victoria M, Querin OM. Review on the modelling of joint behaviour in steel frames. J Constr Steel Res 2011; 67(5):741-758. https://doi.org/10.1016/j.jcsr.2010.12.014

[2] Yee KL, Melchers RE. Moment–rotation curves for bolted connections. J Struct Eng 1986; 112(3): 615-635 https://doi.org/10.1061/(ASCE)0733-9445(1986)112:3(615)

[3] Jaspart JP. Etude de la semi-rigidité des noeuds poutre-colonne et son influence sur la résistance et la stabilité des ossatures en acier. PhD thesis. Belgium: University of Liege; 1991.

[4] C.Faella, V. Piluso, G. Rizzano, Structural Steel Semirigid Joints. CRC Press LLC, Boca Ratón, Florida, 2000.

[5] Lemonis ME, Gantes CJ. Mechanical modeling of the nonlinear response of beam-to-column joints. J Constr Steel Res 2009; 65(4):879-890. https://doi.org/10.1016/j.jcsr.2008.11.007

[6] Lima LRO, Simões da Silva L, Vellasco PCG, Andrade SAL. Experimental evaluation of extended endplate beam-to-column joints subjected to bending and axial force. Eng Struct 2004; 26(10):1333-1347. https://doi.org/10.1016/j.engstruct.2004.04.003

[7] Daniūnas A, Urbonas K. Behaviour of semi-rigid steel beam-to-beam joints under bending and axial forces. J Constr Steel Res 2006; 62 (12):1244-1249 https://doi.org/10.1016/j.jcsr.2006.04.024

[8] Cabrero JM, Bayo E. The semi-rigid behaviour of three-dimensional steel beam-to column

joints subjected to proportional loading. Part II: theoretical model and validation. J Constr Steel Res 2007; 63(9):1254–1267 https://doi.org/10.1016/j.jcsr.2006.11.005

[9] Latour M, Rizzano G, Santiago A, Simões da Silva L. Experimental analysis and mechanical modeling of T-stubs with four bolts per row. J Constr Steel Res 2014; 101:158-174. https://doi.org/10.1016/j.jcsr.2014.05.004

[10] EUROCODE 3, Design of Steel Structures – part 1.8: Design of joints CEN, Brussels, 2005.

[11] Kishi N, Chen WF. Data base of steel column connections. Structural engineering report CE-STR-86-26. West Lafayette, IN: Purdue University, 1986.

[12] Bayo E, Loureiro A, Lopez M, Simões da Silva L. General component based cruciform finite elements to model 2D steel joints with beams of equal and different depths. Eng Struct 2017; 152:698-708. https://doi.org/10.1016/j.engstruct.2017.09.042

[13] De Lima LRO, De Andrade SAL, da S Vellasco PCG, da Silva LS. Experimental and Mechanical Model for Predicting the Behaviour of Minor Axis Beam-to-column Semi-rigid Joints. Int J Mech Sci 200; 44(6):1047-1065. https://doi.org/10.1016/S0020-7403(02)00013-9

[14] Gil B, Goñi R, Bayo E. Initial stiffness and strength characterization of minor axis T-stub under out-of-plane bending. J Constr Steel Res 2018; 140:208-221. https://doi.org/10.1016/j.jcsr.2017.10.028

[15] Daniūnas A, Urbonas K. Analysis of the steel frames with the semi-rigid beam-to-beam and beam-to-column knee joints under bending and axial forces. Eng Struct 2008; 30(11):3114-3118. https://doi.org/10.1016/j.engstruct.2008.04.027

[16] L.G. Lema. (2009) Beam-to-beam joints with bolted end-plate connections concerning steel platforms Angra 2NPP. International Nuclear Atlantic Conference – INAC 2009 Rio de Janeiro, RJ, Brazil, September 27 to October 2.

[17] Hawxwell DA, Tsavdaridis KD.Beam-to-beam eccentric end plate connections - Experimental comparison to fin plate and partial-depth end plate connections. Structures 2019; 19:411-423. https://doi.org/10.1016/j.istruc.2019.02.012

[18] Loureiro A, López M, Gutiérrez R, Reinosa JM. Experimental and numerical analysis of E-stubs in three dimensional joints: A new analytical formulation for the stiffness calculation. Eng Struct 2013; 53:1–9. https://doi.org/10.1016/j.engstruct.2013.03.035

[19] Loureiro A, López M, Gutiérrez R, Reinosa JM. A new analytical formulation for the E-stub strength calculation in three dimensional steel joints with additional plates welded to the weak axis, Eng Struct 2013; 56:2263–2272. https://doi.org/10.1016/j.engstruct.2013.08.037

[20] Gil B, Goñi R, Bayo E. Major axis steel joint with additional plates subjected to torsion: Stiffness characterization, Eng Struct 2020; 220:111021. https://doi.org/10.1016/j.engstruct.2020.111021.

[21] D'Aniello M, Cassiano D, Landolfo R. Simplified criteria for finite element modelling of European preloadable bolts. Steel Compos Struct 2017; 24(6): 643-658. https://doi.org/10.12989/scs.2017.24.6.643

[22] Gantes CJ, Lemonis ME. Influence of equivalent bolt length in finite element modeling of T-stub steel connections, Comput Struct 2003; 81:595-604. https://doi.org/10.1016/S0045-7949(03)00004-X

APPENDIX

The following table collects data of stiffness and resistance of all the models of the parametric study. $k_{ap,FEM}$ and k_{ap} are the value of the stiffness of the additional plate of the finite element model and the equivalent frame, respectively. The error between them is e_k that is presented in percentage. $F_{ap,Rd,FEM}$ and $F_{ap,Rd}$ represent the value of the resistance of the additional plate of the finite element model and the equivalent frame, respectively. The error between them is e_F which is also presented in percentage. Empty cells of resistance in the table occur because the finite element model does not develop completely the plastic range before the yield of the bolts.

In the table, the column called *Ref. Model* is a code to define the geometry of the models that was exposed in Table 4. The first four characters define the type of submodel, which defines the profile of the beams. The fifth character defines the horizontal distance between bolts (w1 or w2). The sixth character defines the vertical distance between bolts (p1 or p2). The seventh character define the thickness of the plate ($t_{ap}1$, $t_{ap}2$ or $t_{ap}3$) and the eighth character defines the type of bolt (10.9TR16 or 10.9TR20). For example, *ME04,2,1,3,2* is a model with a profile type HA300A, the horizontal distance between bolts is 150 mm, the vertical distance between bolts is 220 mm, the thickness of the additional plate is 15 mm and the bolt type is 10.9TR20. (See Table 4).

Ref. Model	$k_{ap,FEM}$ (kN/mm)	k_{ap} (kN/mm)	e_k	$F_{ap,Rd,FEM}$ (kN)	$F_{ap,Rd}$ (kN)	e_F
ME01,1,1,1,1	293	325	11%	109	101	-7%
ME01,1,1,1,2	403	390	-3%	139	122	-12%
ME01,1,1,2,1	381	415	9%	133	125	-6%
ME01,1,1,2,2	482	487	1%	154	147	-4%
ME01,1,1,3,1	472	495	5%	158	147	-7%
ME01,1,1,3,2	572	574	0%	185	171	-8%
ME01,1,2,1,1	126	127	1%	81	74	-9%
ME01,1,2,1,2	150	145	-3%	87	84	-3%
ME01,1,2,2,1	171	184	8%	106	100	-6%
ME01,1,2,2,2	205	208	1%	119	113	-5%
ME01,1,2,3,1	228	241	6%	126	125	0%
ME01,1,2,3,2	255	270	6%	140	140	0%
ME01,2,1,1,1	321	344	7%	123	114	-8%
ME01,2,1,1,2	438	412	-6%	141	135	-4%
ME01,2,1,2,1	421	438	4%	149	139	-6%
ME01,2,1,2,2	532	513	-4%	174	163	-6%
ME01,2,1,3,1	529	523	-1%	180	163	-10%
ME01,2,1,3,2	640	604	-6%	205	188	-8%
ME01,2,2,1,1	140	136	-3%	91	81	-11%
ME01,2,2,1,2	167	154	-8%	101	92	-8%
ME01,2,2,2,1	192	196	2%	114	109	-4%
ME01,2,2,2,2	226	220	-2%	126	122	-3%
ME01,2,2,3,1	257	257	0%	134	137	2%
ME01,2,2,3,2	297	286	-4%	150	152	1%
ME02,1,1,1,1	340	387	14%	140	137	-3%
ME02,1,1,1,2	426	449	5%	155	160	4%
ME02,1,1,2,1	435	471	8%	170	162	-5%
ME02,1,1,2,2	514	539	5%	204	188	-8%
ME02,1,1,3,1	578	587	2%	219	199	-9%
ME02,1,1,3,2	662	661	0%	250	227	-10%
ME02,1,2,1,1	118	120	2%	105	98	-7%
ME02,1,2,1,2	132	133	1%	115	109	-5%
ME02,1,2,2,1	162	166	3%	133	127	-4%
ME02,1,2,2,2	175	183	4%	145	140	-4%
ME02,1,2,3,1	236	239	1%	158	172	9%
ME02,1,2,3,2	253	260	3%	175	188	7%
ME02,2,1,1,1	373	409	10%	160	155	-4%
ME02,2,1,1,2	456	474	4%	179	179	0%
ME02,2,1,2,1	484	498	3%	205	183	-11%
ME02,2,1,2,2	570	568	0%	223	210	-6%
ME02,2,1,3,1	650	620	-5%	255	223	-13%
ME02,2,1,3,2	748	697	-7%	281	252	-10%
ME02,2,2,1,1	136	129	-5%	117	108	-8%
ME02,2,2,1,2	150	142	-5%	127	118	-7%
ME02,2,2,2,1	183	178	-3%	139	139	0%
ME02,2,2,2,2	201	195	-3%	151	152	1%
ME02,2,2,3,1	260	255	-2%	175	188	7%
ME02,2,2,3,2	287	277	-4%	188	204	9%
ME03,1,1,1,1	386	438	14%	148	154	4%
ME03,1,1,1,2	472	509	8%	172	182	6%
ME03,1,1,2,1	483	526	9%	190	181	-5%
ME03,1,1,2,2	588	602	2%	212	210	-1%
ME03,1,1,3,1	650	638	-2%	246	217	-12%
ME03,1,1,3,2	748	718	-4%	262	248	-5%
ME03,1,2,1,1	125	127	2%	101	103	2%
ME03,1,2,1,2	141	140	0%	112	115	3%
ME03,1,2,2,1	173	174	0%	147	133	-10%
ME03,1,2,2,2	190	190	0%	163	147	-10%
ME03,1,2,3,1	244	244	0%	191	177	-7%
ME03,1,2,3,2	263	266	1%	205	194	-6%
ME03,2,1,1,1	423	464	10%	170	178	5%
ME03,2,1,1,2	516	537	4%	195	208	7%
ME03,2,1,2,1	549	556	1%	218	208	-5%
ME03,2,1,2,2	647	635	-2%	241	239	-1%
ME03,2,1,3,1	718	674	-6%	290	247	-15%
ME03,2,1,3,2	839	757	-10%	305	280	-8%
ME03,2,2,1,1	144	135	-6%	115	115	0%
ME03,2,2,1,2	162	149	-8%	121	127	5%
ME03,2,2,2,1	195	185	-5%	159	148	-7%

ME03,2,2,2,2	213	203	-5%	182	162	-11%
ME03,2,2,3,1	282	260	-8%	202	196	-3%
ME03,2,2,3,2	303	282	-7%	219	213	-3%
ME04,1,1,1,1	437	499	14%	158	170	7%
ME04,1,1,1,2	529	581	10%	181	201	11%
ME04,1,1,2,1	536	598	12%	204	199	-2%
ME04,1,1,2,2	658	686	4%	226	233	3%
ME04,1,1,3,1	703	717	2%	-	-	-
ME04,1,1,3,2	828	809	-2%	285	271	-5%
ME04,1,2,1,1	136	137	1%	101	109	8%
ME04,1,2,1,2	152	151	0%	113	121	7%
ME04,1,2,2,1	181	188	4%	138	140	2%
ME04,1,2,2,2	204	206	1%	170	155	-9%
ME04,1,2,3,1	262	264	1%	191	186	-3%
ME04,1,2,3,2	281	287	2%	220	204	-7%
ME04,2,1,1,1	471	527	12%	175	198	13%
ME04,2,1,1,2	576	613	6%	207	232	12%
ME04,2,1,2,1	594	632	6%	237	231	-2%
ME04,2,1,2,2	720	723	0%	258	267	3%
ME04,2,1,3,1	790	758	-4%	-	-	-
ME04,2,1,3,2	925	853	-8%	328	309	-6%
ME04,2,2,1,1	152	146	-4%	118	122	4%
ME04,2,2,1,2	172	161	-7%	127	136	7%
ME04,2,2,2,1	208	201	-4%	168	157	-6%
ME04,2,2,2,2	228	219	-4%	195	173	-11%
ME04,2,2,3,1	301	281	-7%	222	207	-6%
ME04,2,2,3,2	324	305	-6%	239	226	-5%
ME05,1,1,1,1	630	687	9%	-	-	-
ME05,1,1,1,2	706	766	8%	297	295	-1%
ME05,1,1,2,1	787	819	4%	-	-	-
ME05,1,1,2,2	879	904	3%	376	344	-8%
ME05,1,1,3,1	869	894	3%	-	-	-
ME05,1,1,3,2	979	980	0%	430	374	-13%
ME05,1,2,1,1	247	255	3%	209	190	-9%
ME05,1,2,1,2	265	276	4%	213	210	-1%
ME05,1,2,2,1	329	340	3%	270	242	-10%
ME05,1,2,2,2	355	366	3%	281	265	-6%
ME05,1,2,3,1	386	394	2%	308	276	-10%
ME05,1,2,3,2	405	423	4%	317	301	-5%
ME05,2,1,1,1	707	741	5%	291	323	11%
ME05,2,1,1,2	801	825	3%	326	365	12%
ME05,2,1,2,1	895	883	-1%	-	-	-
ME05,2,1,2,2	1001	972	-3%	413	423	2%
ME05,2,1,3,1	996	963	-3%	-	-	-
ME05,2,1,3,2	1124	1054	-6%	-	-	-
ME05,2,2,1,1	280	277	-1%	210	228	9%
ME05,2,2,1,2	300	299	0%	228	249	9%
ME05,2,2,2,1	376	369	-2%	-	-	-
ME05,2,2,2,2	402	396	-1%	313	313	0%
ME05,2,2,3,1	432	428	-1%	-	-	-
ME05,2,2,3,2	471	458	-3%	345	353	2%
ME06,1,1,1,1	940	966	3%	-	-	-
ME06,1,1,1,2	1052	1069	2%	-	-	-
ME06,1,1,2,1	1042	1052	1%	-	-	-
ME06,1,1,2,2	1174	1156	-2%	-	-	-
ME06,1,1,3,1	1144	1125	-2%	-	-	-
ME06,1,1,3,2	1298	1230	-5%	-	-	-
ME06,1,2,1,1	372	377	2%	288	254	-12%
ME06,1,2,1,2	401	406	1%	303	280	-8%
ME06,1,2,2,1	433	438	1%	-	-	-
ME06,1,2,2,2	474	471	-1%	358	317	-11%
ME06,1,2,3,1	496	497	0%	-	-	-
ME06,1,2,3,2	540	531	-2%	396	353	-11%
ME06,2,1,1,1	1029	1033	0%	-	-	-
ME06,2,1,1,2	1164	1141	-2%	-	-	-
ME06,2,1,2,1	1133	1124	-1%	-	-	-
ME06,2,1,2,2	1297	1233	-5%	-	-	-
ME06,2,1,3,1	1238	1201	-3%	-	-	-
ME06,2,1,3,2	1430	1311	-8%	-	-	-
ME06,2,2,1,1	407	406	0%	287	304	6%
ME06,2,2,1,2	434	436	1%	310	331	7%

ME06,2,2,2,1	464	472	2%	-	-	-
ME06,2,2,2,2	510	505	-1%	366	374	2%
ME06,2,2,3,1	524	534	2%	-	-	-
ME06,2,2,3,2	582	570	-2%	409	415	1%
ME07,1,1,1,1	204	207	2%	66	61	-7%
ME07,1,1,1,2	278	246	-11%	74	69	-6%
ME07,1,1,2,1	258	267	3%	78	74	-6%
ME07,1,1,2,2	334	310	-7%	90	82	-9%
ME07,1,1,3,1	322	320	-1%	88	84	-4%
ME07,1,1,3,2	391	366	-6%	108	94	-14%
ME07,1,2,1,1	107	105	-1%	48	43	-10%
ME07,1,2,1,2	134	120	-10%	51	48	-7%
ME07,1,2,2,1	143	148	3%	52	55	6%
ME07,1,2,2,2	171	167	-2%	62	61	-1%
ME07,1,2,3,1	186	190	2%	62	67	8%
ME07,1,2,3,2	210	212	1%	72	73	1%
ME07,2,1,1,1	197	210	7%	64	63	-3%
ME07,2,1,1,2	268	249	-7%	72	71	-2%
ME07,2,1,2,1	247	270	9%	77	75	-2%
ME07,2,1,2,2	322	314	-2%	92	84	-8%
ME07,2,1,3,1	309	324	5%	88	87	-1%
ME07,2,1,3,2	374	371	-1%	106	96	-10%
ME07,2,2,1,1	103	107	3%	47	44	-7%
ME07,2,2,1,2	129	122	-5%	51	49	-5%
ME07,2,2,2,1	139	150	8%	53	57	8%
ME07,2,2,2,2	165	169	3%	62	62	1%
ME07,2,2,3,1	175	192	10%	62	69	11%
ME07,2,2,3,2	201	215	7%	72	75	4%
ME08,1,1,1,1	223	229	3%	75	70	-6%
ME08,1,1,1,2	302	272	-10%	83	80	-3%
ME08,1,1,2,1	281	293	4%	89	84	-6%
ME08,1,1,2,2	363	341	-6%	103	95	-8%
ME08,1,1,3,1	350	347	-1%	98	96	-2%
ME08,1,1,3,2	426	397	-7%	119	106	-11%
ME08,1,2,1,1	90	85	-5%	46	42	-9%
ME08,1,2,1,2	110	97	-12%	51	46	-11%
ME08,1,2,2,1	124	124	0%	51	55	7%
ME08,1,2,2,2	142	138	-3%	60	60	1%
ME08,1,2,3,1	158	161	2%	61	67	10%
ME08,1,2,3,2	182	179	-2%	71	73	3%
ME08,2,1,1,1	217	233	7%	72	73	1%
ME08,2,1,1,2	295	276	-6%	84	83	-1%
ME08,2,1,2,1	273	298	9%	88	88	0%
ME08,2,1,2,2	353	346	-2%	101	98	-2%
ME08,2,1,3,1	338	352	4%	101	99	-2%
ME08,2,1,3,2	411	404	-2%	120	110	-8%
ME08,2,2,1,1	87	87	0%	45	43	-5%
ME08,2,2,1,2	105	98	-7%	51	48	-6%
ME08,2,2,2,1	120	126	5%	52	57	11%
ME08,2,2,2,2	138	141	2%	60	62	4%
ME08,2,2,3,1	152	164	8%	61	70	14%
ME08,2,2,3,2	175	182	4%	71	76	6%
ME09,1,1,1,1	224	232	3%	82	79	-3%
ME09,1,1,1,2	299	276	-8%	93	96	3%
ME09,1,1,2,1	288	306	6%	101	100	-1%
ME09,1,1,2,2	364	357	-2%	119	118	-1%
ME09,1,1,3,1	363	366	1%	113	117	4%
ME09,1,1,3,2	430	419	-3%	139	132	-5%
ME09,1,2,1,1	105	101	-4%	52	54	4%
ME09,1,2,1,2	128	114	-11%	59	59	1%
ME09,1,2,2,1	143	147	2%	77	71	-8%
ME09,1,2,2,2	168	164	-2%	82	77	-5%
ME09,1,2,3,1	186	190	2%	83	86	3%
ME09,1,2,3,2	212	210	-1%	95	93	-2%
ME09,2,1,1,1	225	235	5%	81	82	2%
ME09,2,1,1,2	302	280	-7%	92	99	8%
ME09,2,1,2,1	290	310	7%	102	103	1%
ME09,2,1,2,2	364	361	-1%	118	121	3%
ME09,2,1,3,1	356	371	4%	114	121	6%
ME09,2,1,3,2	430	424	-1%	139	136	-2%
ME09,2,2,1,1	105	102	-3%	52	56	8%

ME09,2,2,1,2	128	116	-10%	59	61	4%
ME09,2,2,2,1	142	149	5%	76	73	-4%
ME09,2,2,2,2	173	167	-3%	83	80	-3%
ME09,2,2,3,1	187	193	3%	83	89	6%
ME09,2,2,3,2	209	213	2%	94	96	2%
ME10,1,1,1,1	213	221	4%	84	84	0%
ME10,1,1,1,2	277	260	-6%	97	102	5%
ME10,1,1,2,1	279	293	5%	111	106	-4%
ME10,1,1,2,2	344	339	-1%	126	126	0%
ME10,1,1,3,1	350	351	0%	132	124	-6%
ME10,1,1,3,2	415	400	-4%	151	145	-4%
ME10,1,2,1,1	61	54	-11%	43	48	12%
ME10,1,2,1,2	72	60	-17%	47	52	11%
ME10,1,2,2,1	88	84	-4%	67	66	-3%
ME10,1,2,2,2	98	92	-6%	73	70	-3%
ME10,1,2,3,1	117	114	-3%	78	82	5%
ME10,1,2,3,2	129	124	-4%	83	88	5%
ME10,2,1,1,1	218	225	3%	85	88	3%
ME10,2,1,1,2	283	264	-7%	100	106	6%
ME10,2,1,2,1	286	298	4%	112	111	0%
ME10,2,1,2,2	352	344	-2%	128	131	2%
ME10,2,1,3,1	358	356	-1%	138	130	-6%
ME10,2,1,3,2	425	405	-5%	153	151	-1%
ME10,2,2,1,1	62	55	-11%	43	50	15%
ME10,2,2,1,2	73	61	-17%	47	54	14%
ME10,2,2,2,1	89	85	-4%	68	68	0%
ME10,2,2,2,2	100	93	-7%	73	73	0%
ME10,2,2,3,1	118	116	-2%	76	85	12%
ME10,2,2,3,2	132	126	-5%	84	91	8%
ME11,1,1,1,1	284	309	9%	120	118	-1%
ME11,1,1,1,2	341	354	4%	137	141	3%
ME11,1,1,2,1	357	387	8%	158	144	-9%
ME11,1,1,2,2	419	439	5%	172	169	-2%
ME11,1,1,3,1	472	477	1%	215	174	-19%
ME11,1,1,3,2	538	532	-1%	210	201	-4%
ME11,1,2,1,1	92	88	-4%	68	77	12%
ME11,1,2,1,2	102	97	-5%	72	85	18%
ME11,1,2,2,1	122	125	2%	96	100	5%
ME11,1,2,2,2	136	135	-1%	108	108	0%
ME11,1,2,3,1	176	177	0%	134	130	-3%
ME11,1,2,3,2	190	190	0%	143	138	-4%
ME11,2,1,1,1	300	316	5%	125	130	4%
ME11,2,1,1,2	360	362	1%	141	153	8%
ME11,2,1,2,1	379	397	5%	164	157	-4%
ME11,2,1,2,2	445	449	1%	179	182	2%
ME11,2,1,3,1	499	488	-2%	216	189	-12%
ME11,2,1,3,2	574	544	-5%	217	217	0%
ME11,2,2,1,1	97	91	-7%	70	82	17%
ME11,2,2,1,2	108	99	-8%	75	91	21%
ME11,2,2,2,1	130	128	-2%	99	107	8%
ME11,2,2,2,2	143	139	-3%	110	115	4%
ME11,2,2,3,1	183	181	-1%	126	139	10%
ME11,2,2,3,2	198	195	-2%	142	147	3%
ME12,1,1,1,1	318	351	10%	124	126	2%
ME12,1,1,1,2	383	403	5%	145	152	4%
ME12,1,1,2,1	400	442	11%	167	154	-8%
ME12,1,1,2,2	470	502	7%	184	183	-1%
ME12,1,1,3,1	525	545	4%	-	-	-
ME12,1,1,3,2	598	609	2%	234	218	-7%
ME12,1,2,1,1	97	96	-2%	71	80	12%
ME12,1,2,1,2	111	105	-5%	75	90	20%
ME12,1,2,2,1	133	136	2%	98	104	6%
ME12,1,2,2,2	146	148	1%	107	117	10%
ME12,1,2,3,1	189	194	2%	143	139	-3%
ME12,1,2,3,2	202	210	4%	158	153	-3%
ME12,2,1,1,1	339	358	6%	130	139	7%
ME12,2,1,1,2	408	412	1%	154	165	7%
ME12,2,1,2,1	430	452	5%	180	169	-6%
ME12,2,1,2,2	505	512	1%	194	198	2%
ME12,2,1,3,1	565	556	-1%	-	-	-
ME12,2,1,3,2	646	621	-4%	243	236	-3%

ME12,2,2,1,1	106	98	-7%	73	85	17%
ME12,2,2,1,2	119	107	-10%	79	96	21%
ME12,2,2,2,1	141	139	-1%	104	111	8%
ME12,2,2,2,2	156	151	-3%	111	124	12%
ME12,2,2,3,1	202	198	-2%	142	149	5%
ME12,2,2,3,2	218	214	-2%	162	162	0%